Fraction of boroxol rings in vitreous boron trioxide

J. Swenson* and L. Börjesson
Department of Applied Physics, Chalmers University of Technology, S-412 96 Göteborg, Sweden
(Received 3 December 1996)

The structure of vitreous boron trioxide (B_2O_3) has been investigated by reverse Monte Carlo modeling using reported neutron and x-ray diffraction data. Structural models with different amounts of borons in boroxol rings were created using coordination and bonding constraints. The structure factors and the corresponding pair correlation functions of the models are generally in good agreement with the experimental neutron and x-ray data. However, the models containing large amounts of boroxol rings show significantly larger deviations from the experimental data than those with small fractions. Furthermore, features of the bond angle and dihedral angle distributions as well as visual inspection of the boroxol-rich models show that most of the rings in these models are seriously distorted from planarity. It is evident that it is not possible to reproduce the experimental neutron structure factor with a high fraction ($>30\%$) of borons in planar boroxol rings. Rather, the results indicate that the structure of vitreous B_2O_3 contains less than 20% borons in boroxol rings. [S0163-1829(97)14517-9]

I. INTRODUCTION

Vitreous boron trioxide (B_2O_3) is a classical glass-forming material and a typical example of a covalently bonded network glass. B_2O_3 is also a key component in many kinds of commercial glasses. During recent years, B_2O_3 has attracted considerable interest as the host glass-forming material in various fast-ion-conducting glasses.[1–8]

The structure of vitreous B_2O_3 has been a much debated issue for many years. Although it is generally accepted that the molecular building block of vitreous B_2O_3 is the planar BO_3 group, the manner in which the BO_3 triangles are connected has long been a matter of controversy.[9–27] The most widely accepted model for the structure of vitreous B_2O_3 was for many years a random network of corner-linked triangles as suggested by Zachariasen.[9] Later, Krogh-Moe combined the results of many spectroscopic investigations and came to the conclusion that the BO_3 triangles prefer to form planar B_3O_6 rings (see Fig. 1),[10] which are connected in a random network structure. Other experimental observations of B_2O_3, such as the sharp Raman vibrational mode at 808 cm^{-1},[11] and specific features in the nuclear magnetic resonance[12] (NMR) and nuclear quadrupole resonance[13] (NQR) spectra, have given support to this model. The suggestion that the Raman vibrational mode at 808 cm^{-1} is due to the ''breathing'' motion of oxygens in decoupled boroxol rings[11] has been supported by calculated vibrational spectra for Bethe lattices of boroxol rings.[14,15] Thus experiments and calculations indicate the presence of boroxol rings in the structure, although the exact ring fraction has been difficult to estimate.

Several structural investigations using diffraction techniques have supported the idea that the structure of vitreous B_2O_3 is built up predominantly by planar B_3O_6 rings.[16–18] However, other interpretations of diffraction data have come to different conclusions.[19–26] The radial distribution functions for simple models containing a mixture of boroxol rings and BO_3 triangles with a variable fraction of boron atoms in boroxol rings were computed by Johnson *et al.*[16] and later by Hannon *et al.*[17] In the work of Johnson *et al.* the results of the models were compared with the experimental real-space correlation function $T(r)$ obtained from neutron diffraction in the range of 0–3 Å. The best agreement was obtained for a model containing 60% of the boron atoms in boroxol rings. In the later work Hannon *et al.* computed the structure factors for models with variable fractions of rings and they were compared to the experimental one. In this case, the best agreement was obtained for a model containing 80% boroxol rings. However, the comparison was only made for local models; there was no requirement to fulfill the experimental density, and only the restricted Q range $5-24$ $Å^{-1}$ was used in the comparison. Thus these two in-

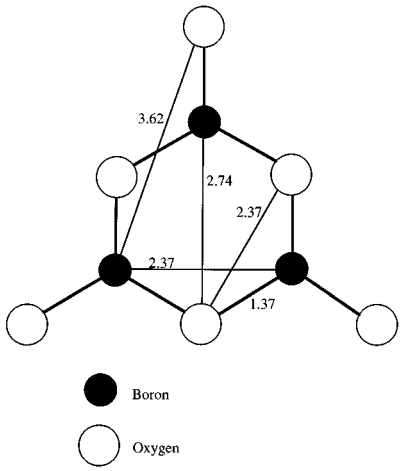

FIG. 1. Schematic illustration of a planar boroxol ring (B_3O_6) with approximate interatomic distances given in angstroms. Note that all the interatomic distances can equally well be obtained by two BO_3 triangles connected in a planar configuration.

vestigations have considered only the relatively short-range order of B_2O_3 and have not taken into account intermediate- and longer-range structural correlations.

Results in favor of non-boroxol-ring models have mainly been obtained from computer simulations, especially using the molecular dynamics (MD) technique. These simulations have produced structures without boroxol rings. However, at least the earlier results have been much questioned, mainly because of the unrealistic bond angle distribution and the inability to reproduce experimental dynamical results and the measured density. It should be noted that recent *ab initio* MD simulations[23,24] and ordinary MD simulations using three- or four-body potentials[25,26] overcome most of these problems without introducing any appreciable amount of boroxol rings.

The aim of this study is to investigate the structure of vitreous B_2O_3 and in particular to test the boroxol ring model using available diffraction data. We apply the reverse Monte Carlo (RMC) simulation technique[28,29] using reported experimental neutron[17] and x-ray data.[19] Models with the correct density and with varying fractions (9–50 %) of boroxol rings are created, which all are in better or equal agreement with the experimental $S(Q)$ compared with the models in Refs. 16 and 17. The models are simultaneously in agreement also with reported x-ray data. The results show that the neutron and x-ray structure factors are relatively insensitive to the fraction of boroxol rings and that there is no particular feature of the structure factors that alone can distinguish between models with a large fraction of boroxol rings and those without rings. The reason for this is the general insensitivity of diffraction data to higher-order correlations than pair correlations, which would be required to describe a six-membered boroxol ring. Furthermore, the main part ($Q > 3\,\text{Å}^{-1}$) of the structure factor is almost entirely determined by short-range correlations. We find, however, by comparing large model configurations whose densities are fixed to the experimental one and using network connectivity constraints, that there are certain structural aspects that can distinguish models of different amounts of boroxol rings.

II. COMPUTATIONAL PROCEDURE

Reverse Monte Carlo simulations[28,29] were used to model the structure of vitreous B_2O_3. The main difference between RMC and ordinary Monte Carlo (MC) simulations is that RMC simulations make use of experimental data instead of interatomic potentials. The MC method minimizes the total potential energy of the system, while the RMC method minimizes the deviation from the experimental diffraction data. Data from different sources [neutron, x-rays, extended x-ray absorption fine structure (EXAFS)] may be combined to create models which simultaneously are in accordance with all the available structural data. In the simulation atoms are moved around in a box in a random way until the calculated diffraction data for the computer configuration agree with the experimental diffraction data. Thus, for the RMC method, no interatomic potential between the particles in the system is required. On the other hand, no dynamical information can be obtained from the RMC method.

In order to obtain starting configurations for the RMC simulations with the desired fraction of boroxol rings and which fulfill bonding constraints, we first ran hard sphere Monte Carlo (HSMC) simulations. The constraints, which were applied to avoid physically unrealistic structures, were of three kinds: closest atom-atom approach, connectivity, and fraction of six-membered rings. The closest distances that two atoms were allowed to approach were determined from experimental results, such as the radial distribution function. The constraints on the B-O network connectivity ensured that all the oxygens were coordinated to two borons and that all the borons were coordinated to three oxygens. The B-O distance was allowed to vary between 1.32 and 1.42 Å, which is consistent with the first peak in the experimental pair correlation function $G(r)$, deconvoluted with the resolution function. It is important that the B-O distance is not allowed to vary too much (i.e., more than the experimentally determined variation), since otherwise the structural features of the boroxol ring model are lost because the rings become completely distorted. The fraction of borons in boroxol rings was chosen to be either unconstrained or constrained to 20%, 30%, and 50%, respectively. The desirable number of rings in the constrained configurations was produced by running a ''ring-counting program.'' When the desirable number of rings and the correct B-O network connectivity were obtained, the applied bonding constraints ensured that the amount of rings was maintained during the simulation. The unconstrained configuration contained 9% boroxol rings, which is the statistical number of six-membered rings in a HSMC-produced structure with no special preference of rings. In all the simulations, the total number of atoms was 2160 and the length of the simulation box was given the value 29.86 Å, which corresponds to the experimentally measured density.

III. RESULTS AND DISCUSSION

The neutron-weighted structure factor, pair correlation function, and bond angle distribution have been computed for the produced RMC structures and compared with the experimental neutron diffraction results. Figure 2 shows the computed neutron-weighted total interference functions $QI(Q)$, in comparison with the experimental interference function (from Ref. 17), for the RMC configurations with the boroxol ring fractions 9%, 20%, 30%, and 50%. All the interference functions of the simulations are in rather good agreement with the experimental interference function, indicating that the neutron data are not particularly sensitive to the fraction of boroxol rings. However, it is obvious that the agreement improves for a decreasing fraction of boroxol rings. This is also seen in the inset of Fig. 3, which shows the root-mean-square (rms) deviations from the experimental structure factor $S(Q)$ [equivalent to $I(Q)+1$], for the four RMC-produced models. It is mainly the higher-Q region (above $8\,\text{Å}^{-1}$) which does not fit to the experimental result for a large fraction of boroxol rings. The most serious difference is that the oscillation is coming out of phase for the highest Q values and that an experimentally found peak at about $16\,\text{Å}^{-1}$ only is reproduced as a shoulder in the RMC simulation. The reason for these deviations will be discussed in the end of this section.

Figure 3 shows the computed x-ray-weighted total interference functions $QI_X(Q)$, in comparison with the experi-

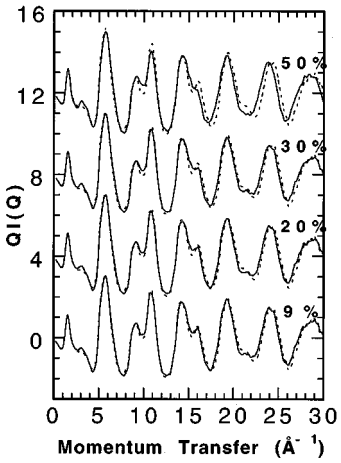

FIG. 2. Computed neutron-weighted total interference functions (solid lines) in comparison with the experimental interference function from Ref. 17 (dashed lines) for the RMC configurations with the boroxol ring fractions 9%, 20%, 30%, and 50%, respectively. The curves have been shifted vertically, in subsequent steps of 4, for clarity.

mental interference function (from Ref. 19), for the same RMC configurations. All the calculated interference functions show some deviations with the experimental interference function. However, it should be noted that the experimental errors are probably relatively large, because there are significant differences between the different published x-ray data of B_2O_3.[18,19,27] Therefore, the comparison with the x-ray data is less significant than with the neutron data. Nevertheless, the rms deviations from the experimental structure factor $F(Q)$ [equivalent to $I_X(Q)+1$] decreases with decreasing fraction of boroxol rings (see the inset of Fig. 3).

Next, we turn to the real-space correlations of the different models. In Fig. 4 we compare the neutron-weighted

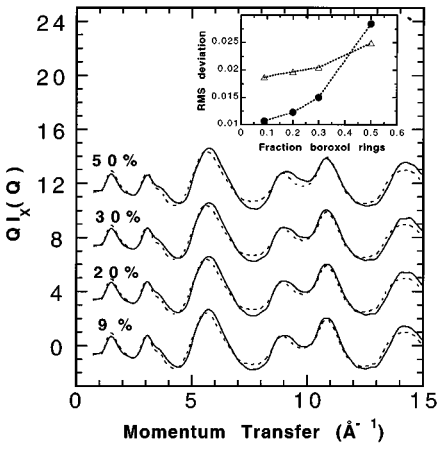

FIG. 3. Computed x-ray-weighted total interference functions (solid lines) in comparison with the experimental interference function from Ref. 19 (dashed lines) for the RMC configurations with the boroxol ring fractions 9%, 20%, 30%, and 50%, respectively. The curves have been shifted vertically, in subsequent steps of 4, for clarity. The inset shows the root-mean-square (rms) deviations from the experimental neutron (●) and x-ray (△) structure factors for the same configurations.

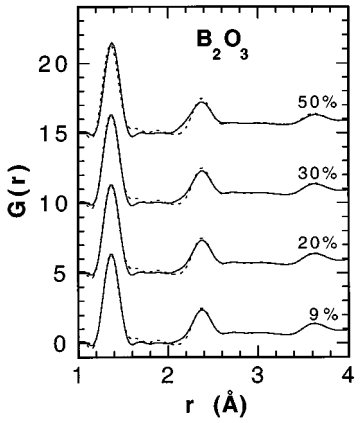

FIG. 4. Computed neutron-weighted atomic pair correlation functions for the RMC models containing 9%, 20%, 30%, and 50% boroxol rings (solid lines) compared with the experimental neutron-weighted atomic pair correlation function (dashed lines). The curves have been shifted vertically, in subsequent steps of 5, for clarity.

atomic pair correlation function $G(r)$ of the Fourier transformed experimental $S(Q)$ data[17] with those calculated for the RMC models containing 9%, 20%, 30%, and 50% boroxol rings, respectively. To ensure proper comparisons, also the calculated atomic pair correlation functions were obtained by Fourier transformation of their corresponding structure factors instead of calculated directly from the corresponding configurations (i.e., the direct calculated atomic pair correlation functions were first Fourier transformed to structure factors and then backtransformed to atomic pair correlation functions again). It is evident from the models containing boroxol rings that a large fraction of boroxol rings gives a slight shift of both the first and second peaks. The first peak shifts to a higher r value, while the second is shifting to a lower r value. This indicates that the average B-O-B and/or O-B-O bond angles are too low. It is also interesting to note that the relatively sharp peak at about 3.6

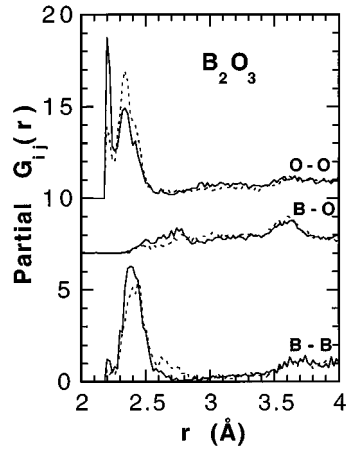

FIG. 5. Partial atomic pair correlation functions $G_{BB}(r)$, $G_{BO}(r)$, and $G_{OO}(r)$ in the r region 2–4 Å, calculated from the models containing 9% (dashed lines) and 50% (solid lines) boroxol rings, respectively. The upper two curves have been shifted to higher values for clarity.

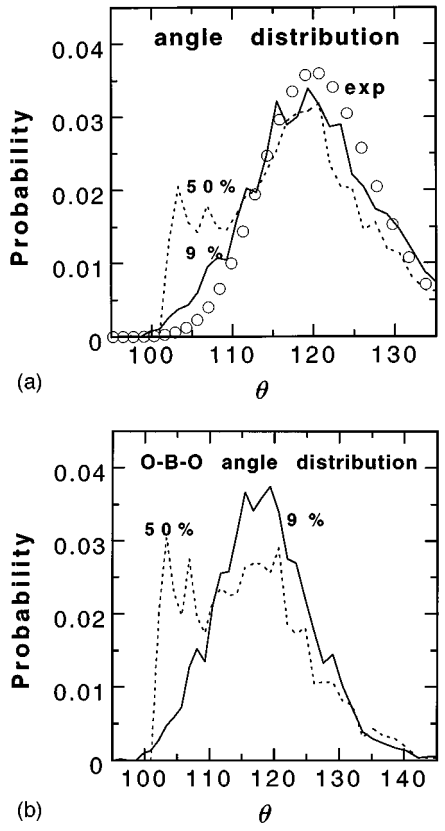

FIG. 6. Bond angle distributions. (a) shows total bond angle distributions (O-B-O+B-O-B) calculated from the experimental $G(r)$ (deconvoluted with the resolution function) (circles) and the models containing 9% (solid line) and 50% (dashed line) boroxol rings, respectively. (b) shows the distribution of O-B-O angles for the models containing 9% (solid line) and 50% (dashed line) boroxol rings, respectively.

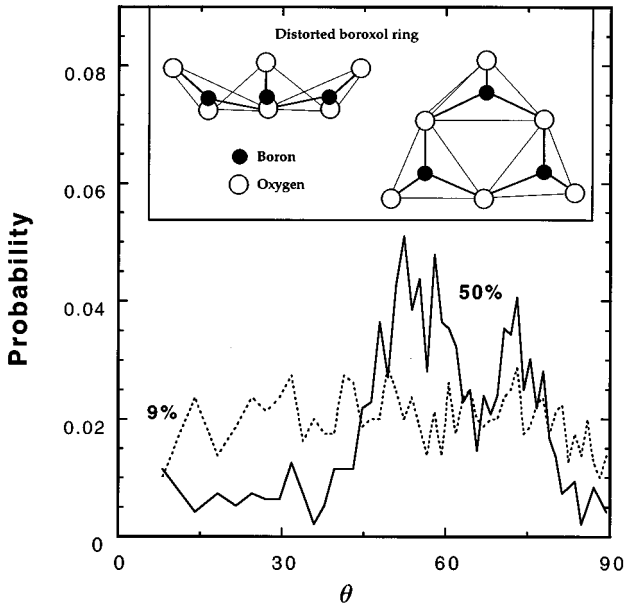

FIG. 7. Dihedral angle distributions between interconnected BO_3 triangles calculated from the models containing 9% (dashed lines) and 50% (solid lines) boroxol rings, respectively. The inset shows an illustration of a distorted boroxol ring (B_3O_6) viewed in the plane (left) and perpendicularly to the plane (right) of the ring. The distorted boroxol ring was found in the RMC-produced models with large amounts of boroxol rings. The oxygens connecting from the distorted boroxol ring are considerably out of the ring plane.

Å is perfectly reproduced in the model containing 9% boroxol rings, while it is slightly too low in the model containing 50% boroxol rings. In Ref. 17 it was proposed that this peak is due to the second B-O distance between an oxygen outside a boroxol ring and a boron within the boroxol ring (see Fig. 1) and, furthermore, that the well-defined planar boroxol ring was the reason for the sharpness of the peak. However, the peak at 3.6 Å is not unique for structures involving boroxol rings. It can equally well be obtained by, for example, two BO_3 triangles connected in a planar configuration,[19] which also the present results show. The presence of nondistorted planar boroxol rings would also produce a sharp peak at about 2.74 Å, corresponding to the diagonal B-O distance in Fig. 1. However, there is only a weak shoulder present at about 2.8 Å in the experimental and the calculated $G(r)$. Furthermore, one should note that a peak at 2.74 Å is also expected for two adjacent BO_3 triangles connected in a planar configuration. Thus there is no unique feature in $G(r)$ that easily can be used to distinguish models with or without boroxol rings.

Figure 5 shows the r region 2–4 Å of the partial atomic pair correlation functions $G_{BB}(r)$, $G_{BO}(r)$, and $G_{OO}(r)$ calculated from the models containing 9% and 50% boroxol rings, respectively. These partial atomic pair correlation functions were calculated directly from the corresponding model configurations. The most significant difference between the two models is in the r region between 2.5 and 2.8 Å. The model containing 50% boroxol rings gives a broad peak around 2.7 Å in $G_{BO}(r)$, which is almost absent in the model containing 9% boroxol rings. This peak is mainly due to the second B-O distance within the boroxol ring (the diagonal in Fig. 1) origin, a planar arrangement of two neighboring BO_3 triangles. The large width of the peak indicates, however, that the boroxol rings in the 50% model are rather distorted. The large difference between the two models in this region of $G_{BO}(r)$ is not clearly seen in the total $G(r)$ because the higher contribution of $G_{BO}(r)$ for the model containing 50% boroxol rings is compensated by a lower (almost zero) contribution of $G_{BB}(r)$ (see Fig. 5). Unfortunately, there is no direct experimental determination of $G_{BO}(r)$, and it is therefore impossible to decide which model is correct from this feature alone.

Figure 6(a) shows total bond angle distributions of O-B-O and B-O-B calculated from the experimental $G(r)$ (deconvoluted with the resolution function) and the models containing 9% and 50% boroxol rings, respectively. However, it should be noted that the experimental bond angle distribution is approximate, since it was calculated with the assumption that the O-B-O and B-O-B bond angle distributions are the same. The results show that the bond angle distribution for the model containing 9% boroxol rings is only slightly shifted to a lower average bond angle compared to the experimental value of 120°, while the model containing 50% boroxol rings shows a clear shift of the bond angle distribution to a lower average value relative to the value of the experimental dis-

tribution. In particular, the boroxol-rich model shows a significant shoulder at about 105°, which is absent in the experimental distribution. In Fig. 6(b) it is seen that this shoulder is mainly related to the O-B-O angles. Considering the shapes and positions of the first and second peaks in the experimental $G(r)$, the O-B-O shoulder occurs at unrealistically low angles, which also the shifts of the peaks in the calculated $G(r)$ show (see Fig. 4). The reason for the too low average O-B-O bond angle of the boroxol-rich model is found in Fig. 7, where the dihedral angle distributions between interconnected BO_3 triangles are shown for the models containing 9% and 50% boroxol rings, respectively. The figure shows that the dihedral angle distribution for the model containing 9% boroxol rings is almost flat; i.e., the distribution is effectively random. This is, however, not the case for the boroxol-rich model, which clearly shows two pronounced peaks at about 53° and 72°, respectively. By close inspection of the computer configuration, it was found that the origin of the peak at 53° is the same as the origin of the O-B-O shoulder at 105°. Both features are due to ''bent'' boroxol rings; i.e., the three oxygens connecting out from a boroxol ring are considerably out of the plane of the ring. In addition, the inner rings of bonds of the boroxol rings are often significantly distorted. A schematic illustration of such a seriously distorted boroxol ring is shown in the inset of Fig. 7. The peak at 72° involves two BO_3 triangles of which at least one of them is situated outside the boroxol rings. The applied constraints would not allow such a large distortion from two triangles in a boroxol ring. Nevertheless, it is evident that the applied constraints of the boroxol-rich model allow the rings to be unrealistically distorted. The allowed variations of the different interatomic distances within the boroxol ring (see Fig. 1) are, for example, about a factor of 2 more than in the models created by Johnson *et al.*[16] The reason for our looser constraints is that we wanted to use constraints that are compatible with the experimentally determined average variation of bond distances for all bonds, this in order to avoid the possibility that the results were dependent on the tightness of the applied constraints instead of the fraction of rings. However, it is likely that the interatomic correlations within the boroxol rings are more well defined than the widths of the corresponding peaks in total $G(r)$. With tighter applied constraints the agreement with the experimental structure factors is much worse.

The question is why the ''strange'' bond and dihedral angle distributions shown in Figs. 6 and 7, respectively, are produced in the model containing 50% boroxol rings. Considering only the short-range order, there is no obvious reason, since the calculated nearest interatomic distances would agree better with the experimental values if the average bond angle was 120° and if boroxol rings were perfectly planar. Instead, the odd features in the bond and dihedral angle distributions and the shifted peaks in $G(r)$ are induced by the requirements of the models to simultaneously reproduce the short- and intermediate-range order, the bonding constraints, and the correct density. The distortions can then be regarded as ''compensation effects'', i.e., configurations with large amounts of planar boroxol rings would tend to have a lower density and the rings have to distort out of the plane in order to fulfill the density constraint. Thus it is the combination of correct density, connectivity, and intermediate-range order that cannot be reproduced in the boroxol-rich model. The structural models in Refs. 16 and 17 do not include the constraints of correct density and reproduced intermediate-range order and, therefore, have all possibilities to reproduce the features of the short-range order with a high fraction of boroxol rings.

From the present results it is not possible to give the exact amount of borons in boroxol rings. However, it is obvious that the agreement with the experimental data improves for decreasing amount of rings and that the errors for the 50% model are larger than the experimental errors in the neutron data. It is also evident how the fraction of distorted rings compared to the total number of rings increases with increasing amount of rings. The high fraction of distorted rings in the 30% and 50% models shows that the experimental density and intermediate-range order of B_2O_3 are not compatible with such high amounts of planar boroxol rings. Rather, the improved planarity of the rings and agreement with the experimental data for decreasing amount of rings indicate that the structure of B_2O_3 contains less than 20% borons in boroxol rings. The model containing 9% rings should be a good representation of the structure of vitreous B_2O_3, since it shows no sign of any significantly distorted rings and the agreement with the experimental neutron and x-ray structure factors is within the experimental errors.

IV. CONCLUSIONS

RMC simulations of vitreous B_2O_3 show that model configurations with large amounts of boroxol rings, built in by constraints, give worse fits to the experimental neutron- and x-ray-weighted interference functions than a model with a small amount of boroxol rings. There are, however, no particular features of the interference functions that can distinguish between the models of different amounts of boroxol rings. In spite of this, the boroxol-rich models exhibit certain features that are not compatible with the experimental data; in particular, the average bond angle is shifted to a lower value due to shifts of the first and second peaks in $G(r)$ to a higher respective lower r value. These shifted peaks in $G(r)$ and the wrong bond angle distribution are produced in the RMC simulation to ''compensate'' other more serious errors in the boroxol ring model. The main flaw of the boroxol-ring-rich models is that in order to satisfy the experimental density and the structure factor the B_3O_6 rings have to distort seriously, giving a dihedral angle distribution between BO_3 triangles in the ring which is incompatible with the definition of planar boroxol rings. Thus the present results show that extreme care must be applied to draw conclusions from different models that only consider the short-range order and which do not have the correct density, although they may give ''reasonable agreement'' with diffraction data. To conclude, the results indicate that the structure of vitreous boron trioxide contains less than 20% of boroxol rings.

ACKNOWLEDGMENTS

We are grateful to Dr. Robert McGreevy for stimulating discussions and for providing the RMC simulation program. This work was financially supported by the Swedish Natural Science Research Council.

*Current address: Department of Physics and Astronomy, University College London, London WC1E 6BT, United Kingdom.
[1] A. Schiraldi and E. Pezzati, Mater. Chem. Phys. **23**, 75 (1989); A. Schiraldi, E. Pezzati, P. Beldani, and S. W. Martin, Solid State Ionics **18 & 19**, 426 (1986).
[2] F. Rocca, G. Dalba, and P. Fornasini, Mater. Chem. Phys. **23**, 85 (1989).
[3] C. Chiodelli, A. Magistris, M. Villa, and J. L. Bjorkstam, J. Non-Cryst. Solids **51**, 143 (1982).
[4] G. Carini, M. Cutroni, A. Fontana, G. Mariotto, and F. Rocca, Phys. Rev. B **29**, 3567 (1984).
[5] L. Börjesson, L. M. Torell, and W. S. Howells, Philos. Mag. B **59**, 105 (1989).
[6] L. Börjesson, L. M. Torell, U. Dahlborg, and W. S. Howells, Phys. Rev. B **39**, 3404 (1989).
[7] H. L. Tuller and D. P. Button, in *Transport-Structure Relations in Fast Ion and Mixed Conductors*, edited by F. W. Poulsen, N. Hessel-Andersen, K. Clausen, S. Skaarup, and O. Soerensen (Risø National Laboratory, Roskilde, Denmark, 1985), p. 119.
[8] A. C. M. Rodrigues, A. Kone, and M. J. Duclot, in *Transport-Structure Relations in Fast Ion and Mixed Conductors*, edited by F. W. Poulsen, N. Hessel-Andersen, K. Clausen, S. Skaarup, and O. Soerensen (Risø National Laboratory, Roskilde, Denmark, 1985), p. 249.
[9] W. H. Zachariasen, J. Am. Chem. Soc. **54**, 3841 (1932).
[10] J. Krogh-Moe, J. Non-Cryst. Solids **1**, 269 (1969).
[11] F. Galeener, G. Lucovsky, and J. C. Mikkelsen, Jr., Phys. Rev. B **22**, 3983 (1980).
[12] G. E. Jellison, Jr., L. W. Panek, P. J. Bray, and G. B. Rouse, Jr., J. Chem. Phys. **66**, 802 (1977).
[13] S. Garvina, P. J. Bray, and G. L. Petersen, J. Non-Cryst. Solids **123**, 165 (1990).
[14] M. A. Kanehisa and R. J. Elliott, Mater. Sci. Eng. B **3**, 163 (1989).
[15] R. A. Barrio, F. L. Castillo-Alvarado, and F. L. Galeener, Phys. Rev. B **44**, 7313 (1991).
[16] P. A. V. Johnson, A. C. Wright, and R. N. Sinclair, J. Non-Cryst. Solids **50**, 281 (1982).
[17] A. C. Hannon, David I. Grimley, Robert A. Hulme, Adrian C. Wright, and Roger N. Sinclair, J. Non-Cryst. Solids **177**, 299 (1994).
[18] R. L. Mozzi and B. E. Warren, J. Appl. Cryst. **3**, 251 (1970).
[19] E. Chason and F. Spaepen, J. Appl. Phys. **64**, 4435 (1988).
[20] F. M. Dunlevey and A. R. Cooper, Bull. Am. Ceram. Soc. **51**, 374 (1972).
[21] S. R. Elliott, Philos. Mag. B **37**, 435 (1978).
[22] G. N. Greaves and E. A. Davis, Philos. Mag. **29**, 1201 (1974).
[23] Hong-Zhang Zhung, Xian-Wu Zou, Zhun Zhi Jin, and De-Cheng Tian, Phys. Rev. B **52**, 829 (1995).
[24] M. P. Teter (unpublished).
[25] A. H. Verhoef and H. W. den Hartog, J. Non-Cryst. Solids **146**, 267 (1992).
[26] R. Fernandez-Perea, F. J. Bermejo, and M. L. Senent, Phys. Rev. B **54**, 6039 (1996).
[27] G. Paschina and G. Piccaluga, J. Chem. Phys. **81**, 6201 (1984).
[28] R. L. McGreevy and L. Pusztai, Mol. Simul. **1**, 359 (1988).
[29] D. A. Keen and R. L. McGreevy, Nature **344**, 423 (1990).